scientific reports

Check for updates

OPEN

Synthesis of composites with nanoscale silicon and silicate oxides with lithium using three-dimensionally driven ball mill

Norihiro Shimoi✉, Hirotaka Aonuma & Masae Komatsu

To achieve high-performance electrochemical anodes properties, active materials of anodes with improved cycle performance were composited using Cu alloys, silicon oxides and Li compounds within a composite by a simple mechanochemical milling process. The three-dimensionally driven ball mill used as a mechanochemical apparatus in this study can independently control two axes and can perform combined milling and frictional movements realized by adjusting the rotational speed of the vessel. The composite consisting of silicon, lithium oxide and copper oxide using these movements has Si nanoparticles, amorphous silicon monoxide, and Si–Cu alloy compounds, and a layer of silicon oxide on its surface. The prepared composite achieved higher retention capacity, higher coulomb efficiencies of approximately 90% and longer-cycle performance than Si particles, indicating a considerable optimisation of electrical and ionic conductivities in the composite. As a result, the method developed enabled the control of Li content to compensate for the lack of Li ions in the composite and optimised cycle performance with Cu alloys, oxides and Li compounds in the composite.

Si-based Li-ion batteries (LIBs) have great potential owing to the higher capacity of Si-based anodes than of current graphite anodes[1]. However, a major obstacle to achieving a satisfactory reversible capacity in practical use is the large change in Si volume observed during charge–discharge operation[2–6] and the irreversible formation of a Si–Li component. Many researchers have attempted to overcome these problems by using nanostructures[4,7–14] or through approaches such as partial oxidation[7,15,16], composite formation with other materials[7,9,11,17–20], liquid-phase synthesis, and various battery production methods. Improvements in the stability of the prepared Si anodes have been observed because of these attempts, leading to an improvement in LIB performance. Although there have been many reports of attempts to optimize both electrical and ionic conductivities[21–25] to the best of our knowledge, there have been no attempts to synthesise active materials that include Li ions to maintain the high performance of an LIB lacking Li ions for charge–discharge characteristics. We consider that further significant improvement may be obtained from the synergistic effects of two or more approaches simultaneously introduced in a simple operation. We propose a method of synthesizing a composite with active Li compounds to compensate for the lack of Li ions in the anode of an LIB system, along with Li–Si or other metal–Si alloys to optimize the electrical and ionic conductivities, by a simple mechanochemical grinding process. Accordingly, we have reported the optimization of the cycling properties of an active Si anode by employing a composite of Si, lithium oxide (Li_2O), and copper oxide (CuO) that were formed by a simple grinding process with a planetary ball mill[26], and the synthesis of single-crystal Si particles covered with silicon monoxide and sub-oxide-rich oxidation films[22].

Thus, we were able to develop an ideal active material structure of the silicon anode satisfying charge–discharge capacity and cycle properties. However, there are still cost disadvantages of the methods currently used to synthesise nanocrystalline structures of silicon and silicon oxides and silicon oxide films coating around composite structures in a single process. Therefore, we attempted to develop a simple method of synthesizing active material particles with a mixture of silicon and silicon-oxide nanoparticles and a silicon mono-oxide film-coated structure based on a mechanochemical method. In this paper, we report the results of synthesizing active materials with both structures described above using a three-dimensionally driven ball mill.

Department of Electrical and Electronic Engineering, Tohoku Institute of Technology, 35-1 Yagiyama Kasumi-cho, Taihaku-ku, Sendai 982-8577, Japan. ✉email: n-shimoi@tohtech.ac.jp

Fig. 1. (a) Three-dimensionally driven ball mill machine. Crushed solids are fed into the spherical container in the centre of the machine. (b) Image of driving a ball mill vessel.

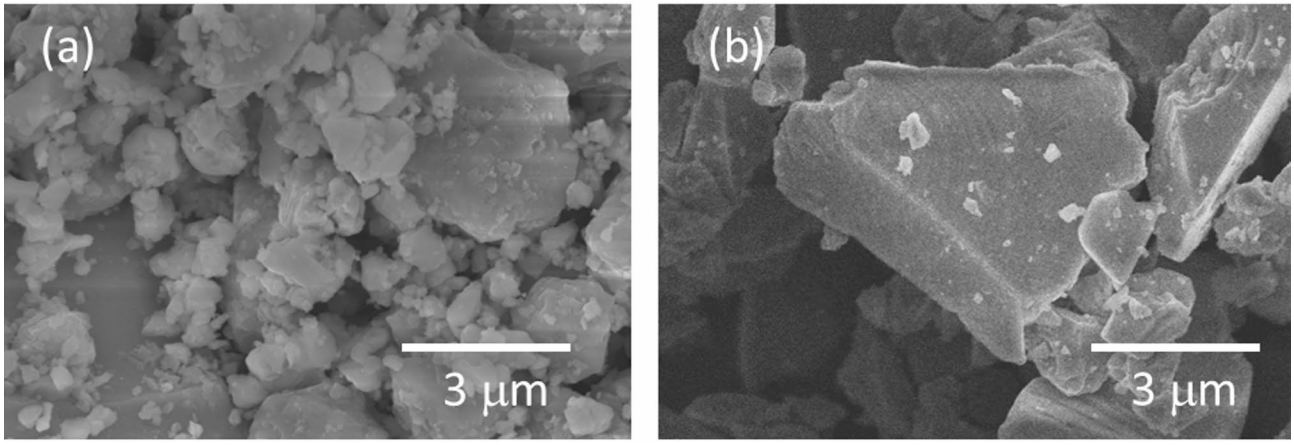

Fig. 2. (a) SEM image of aggregates of composite with Si, CuO, and Li_2O particles. (b) Si particles before grinding by three-dimensionally ball mill as a reference.

Experimental procedure

Composite with Si, Li_2O, and CuO particles

A mixture of Si, Li_2O, and CuO particles (2.0 g, 10:0.25:0.75 Si to oxide atoms in Li_2O and CuO), each of which had an average diameter of 4 μm (Kojundo Chemistry Laboratory Co., Ltd., Japan), was put in a zirconia mill pot (250 cm^3 inner volume) with 20 zirconia balls. The mixture was ground using a three-dimensionally driven ball mill (HYPER SHAKER, Kameyama Iron Factory Inc., Japan). The machine controls the horizontal and vertical axes independently to rotate the vessel three-dimensionally at a high speed and crush, mix and agitate the mixture uniformly, as shown in Fig. 1. The process is expected to be shorter than that using a conventional ball mill and the extent of internal temperature increase is lower, making the machine effective for grinding samples such as organic materials, for which the effects of heat should be minimised. In this study, we set both the horizontal and vertical rotation speeds to 600 rpm. The powder was pre processed for 3 h with the mill vessel filled with argon gas to produce the aggregates of the composite with Si, Li_2O, and CuO, followed by 45 min of milling in air at a speed of 250 rpm. The rotation speeds of 600 rpm with argon gas and 250 rpm in air were determined based on the rotation speed dependence of the initial discharge capacity shown in Figs. S1 and S2 of Supporting data.

Preparation of composite electrodes

The composites with Si, Li_2O, and CuO in Fig. 2 were prepared as follows. The prepared composite was mixed with a binder composed of polyamic acid (Ube-kousan KK Company, Japan) and acetylene black (AB; Denkikagaku, Japan) as a conductive material in a 1-methyl-2-pyrrolidone (NMP) solution. The Si composite: binder: AB weight ratio was 70:20:10. The slurry of the electrode components was cast onto a Cu foil and dried at 70 °C for 20 min in air. The cast electrodes were cut to a diameter of 10 mm. The obtained electrodes had

thicknesses in the range of 40–50 µm. The electrodes were further dried at 550 °C under vacuum for 3 h and then pressed at 200 kgf/cm. The specific capacity was calculated according to the weight of the composite/binder/AB. Electrochemical tests of the composite electrodes were conducted using two-electrode test coin cells (type 2032; Housen, Japan) with a separator, and a gasket to hold the electrode.

Assembly of test coin cell for LIB

The coin cells were assembled in an Ar-filled glove box using 1 M hexafluorophosphate ($LiPF_6$) in a solution of ethylene carbonate (EC), diethylene carbonate (DEC), and dimethyl carbonate (DMC) (60:25:15, v/v) as the electrolyte. For high-charge–discharge operations, a $LiCoO_2$-coated film (300 µm thick) at a capacity of 12.0 mAh/cm^2 was employed as the cathode counter electrode, whereas a metal Li foil was employed for impedance measurement. The separator was a polyethylene/polypropylene/polyethylene multi stacked film with a thickness of 10 µm. The electrochemical performance of the two-electrode coin cells was evaluated using a potentiostat (Hokuto-denko Co., Ltd., Japan).

Results and discussion

Preparation of composite

Mechanochemical phenomena have been widely studied[27–29]. One line of research has focused on mechanochemical reduction employing one element and one compound[30,31], such as the reduction of CuO by grinding it with Al, Mg, or Si to form Cu powders[32]. However, the products obtained from equimolar CuO and Si fail to achieve high LIB performance because the presence of a Si oxide, probably SiO_2, synthesized by the mechanochemical process, leads to excessive oxide atoms in Si; therefore, the composite does not function as an active material. In contrast, at a molar ratio of 10:0.75, Si was expected to be partially oxidized by the oxide atoms in CuO, producing a composite with excellent LIB performance. Furthermore, the mechanochemical reactions between Si and Li_2O when mixed at a molar ratio of 10:0.25 (Si: O) are expected to produce a composite through a non-equilibrium active reaction[26]. Li has lower electronegativity than Si and Cu, which are formed by mechanochemical reactions[32] and inhibit the reactions of oxide atoms, and Li metals are less likely to be mechanochemically synthesised. Figure 2 shows images of the aggregate's composites with Si, CuO and Li_2O particles.

The X-ray diffraction (XRD; Rigaku Co., Ltd., Japan) patterns in Fig. 3 show the crystallinity of components of the composite obtained by the mechanochemical grinding of Si, Li_2O, and CuO particles. The oxide atoms in

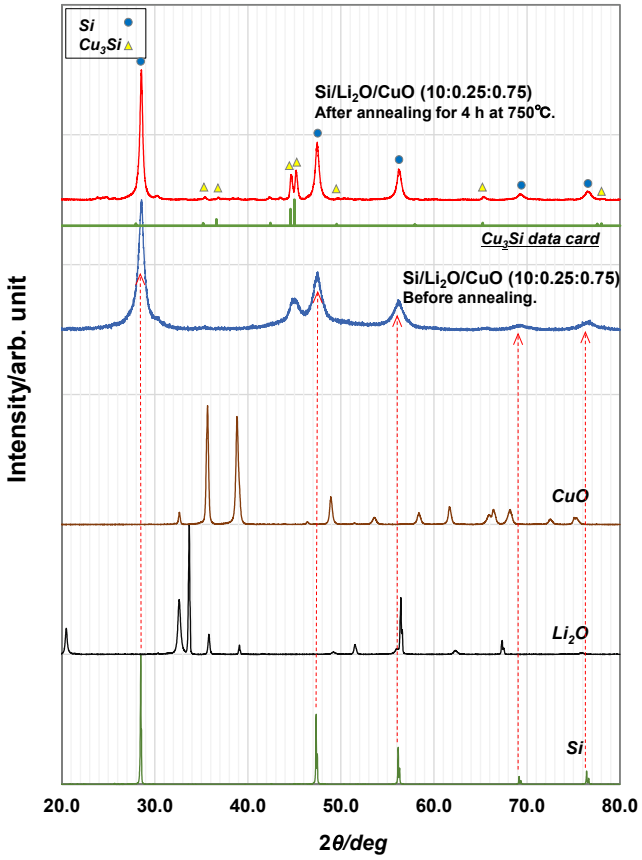

Fig. 3. XRD patterns of composite with Si, Li_2O, and CuO particles and each raw material before grinding.

CuO are reduced, and residual Cu is expected to form an alloy with Si[27]. The Si grain size in the composite after annealing for 4 h at 750 ℃ was calculated to be approximately 30 nm from the peak half-width of Si(110) in Fig. 3. The Cu–Si alloy is in the form of Cu_3Si[33] and acts as a current collector. This alloy is electrically conductive and an important material for realizing higher charge–discharge characteristics, but it does not function as an active material, and there were no peaks originating from CuO and Li_2O. Thus, the compounds synthesized from the reduction and oxidation of CuO or Li_2O were amorphous in the prepared composite.

Figure 4 shows scanning transmission electron microscopy (STEM; Hitachi High-Technologies Co. Ltd., Japan) images of the prepared composite. The cross-sectional STEM images in Fig. 4a, b show the dark-field STEM images of an anode electrode film. Moreover, Fig. 4b shows a dark-field STEM image of the area encircled in red in Fig. 4a. The dark grey areas in these images correspond to the Si, Li, and oxide atoms, whereas the bright grey areas correspond to Cu_3Si in the composite[26]. The crystal lattices indicate the orientation of each nanoscale Si or Cu_3Si crystal lattice in Fig. 4c. The high-resolution STEM images in Fig. 4c confirm that each grain has a random crystal orientation and that the composite mainly comprises polycrystalline Si with nanoscale grains of approximately 40 nm φ on average, Cu_3Si nanoscale grains, and other amorphous materials including a Li–silicate oxide compound. Thus, the Si, Li_2O, and CuO particles were confirmed as aggregates of nanoscale grains based on Si, Cu_3Si, and other materials.

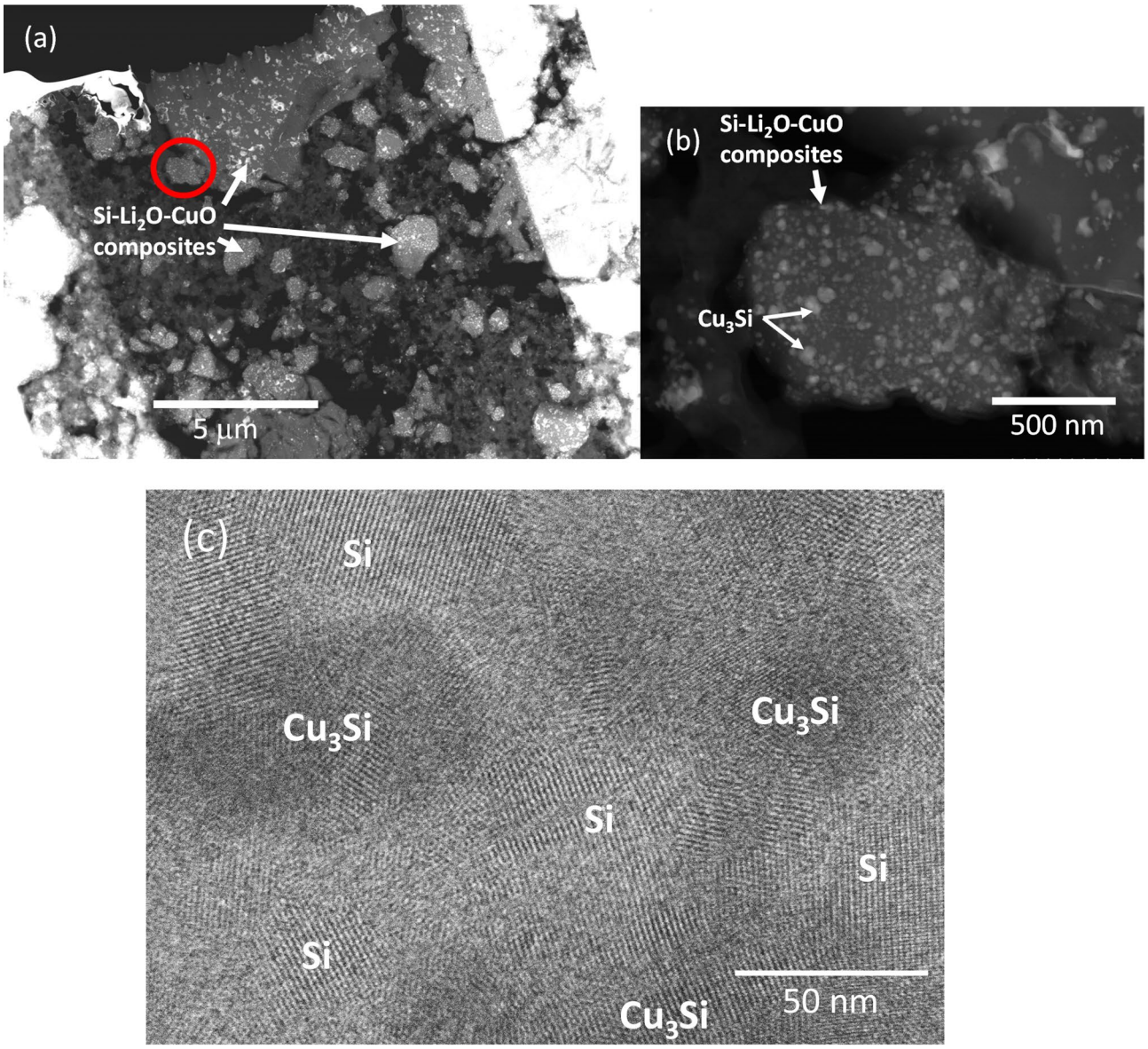

Fig. 4. STEM images of the composite with Si, Li_2O, and CuO particles. **(a)** Cross-sectional STEM image of the composite. **(b)**, **(c)** Enlarged STEM images of the area encircled in red in **(a)**. Black dots in **(c)** indicate Cu_3Si alloy grains in the composite.

The structure of the composite is hypothesized to include nanoscale Si grains, which prevent the cracking of Si anodes after numerous repetitions of the charge–discharge cycle[10,13], Cu_3Si as a current collector, and amorphous silicon oxide (SiO) surrounding each Si grain.

Figure 5 shows cross-sectional images of the synthesized particle boundary area for compositional analysis energy dispersive X-ray spectroscopy (EDX). Figure 5b shows the distribution of Si, Cu and O elements in the measurement area in Fig. 5(a). The EDX results showed that the atomic concentration ratio of Si to O was 10:1.13. The oxygen concentration is higher than the designed composition ratio, but this may be due to the synthesis process in air. Moreover, it can be seen that O is particularly localised at around 30 nm near the surfaces of the particles. It is assumed that the silicon oxide film is synthesized on the surface layer of the composite, as the surface of the natural oxide film is stabilised after being formed to a thickness of 10–100 nm and no further formation occurs. Moreover, Fig. 6a shows a STEM image of the area near Fig. 5. To analyze detail elements of silicon and oxide, spot tests were performed for silicon and oxygen along the white arrow in the figure. Figure 6b shows the composition distribution of silicon and oxygen obtained by EDX. It confirms that a film mainly composed of SiOx was formed on the Si-Li_2O-CuO composite surface.

Electrochemical properties of prepared composite

To experimentally obtain good charge–discharge properties, LIB negative electrodes were prepared on Cu foil by mixing Si, Li_2O and CuO at an atomic ratio of 10:0.25:0.75[26]. The samples evaluated were synthesised only in Ar gas atmosphere, and synthesised in air after argon gas injection, and electrodes with only silicon powder were prepared as a reference. Moreover, the charge–discharge properties of these samples were evaluated. Figure 6a shows the electrochemical performance of the composite anode evaluated in a 2032-type coin cell with metallic lithium foil in a constant-current charge–discharge test in the voltage range of 0.02–3.2 V and a loading current density of 3.2 mA/cm^2 (1 C) at 300 K. The battery was charged at 100%. In the synthesis of the anode active material, the initial and second charge–discharge curves in Fig. 7a are shown for the argon gas atmosphere only and the air injection sample. On the other hand, the initial charge–discharge curves are also shown for the raw sample with silicon powder as a reference. The results indicate that the charge and reversible discharge capacities depend on the components of the active material. The prepared composite synthesized in Ar atmosphere and air, indicated by the orange solid line, exhibited an initial coulombic efficiency of 95% at a current density of 3.2 mA/cm^2 (1 C), as shown in Fig. 7a. The red single-point line and blue dotted line indicate that the initial coulombic efficiencies were 89.2% and 70.3% at a current density of 3.2 mA/cm^2 (1 C), respectively. The initial coulombic efficiency, which is calculated using the charging capacity at 2.5 V, of the active Si material in the LIB was around 70%; however, the prepared composite attained an initial coulombic efficiency of more than 89% with a high

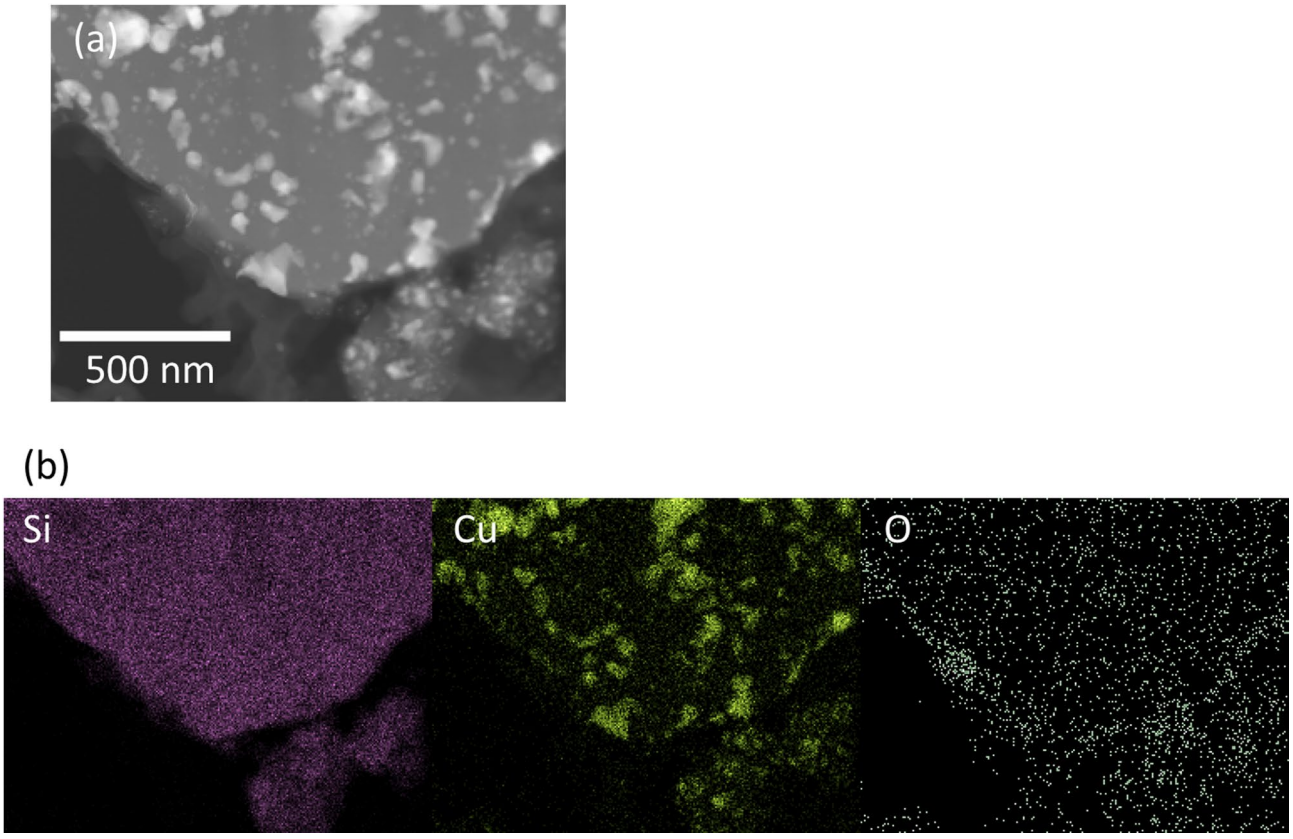

Fig. 5. (a) Cross-sectional EDX image of the composite with Si, Li_2O, and CuO particles. (b) EDX images of distribution of Si, Cu, and O elements.

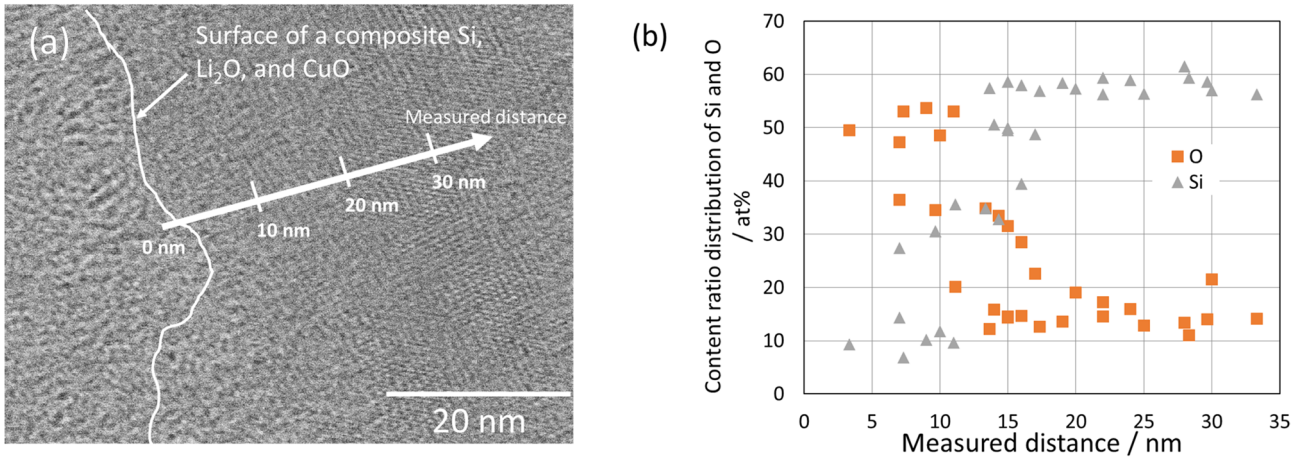

Fig. 6. STEM image of surface of a Si-Li_2O-CuO composite in area near a particle in Fig. 5, and (b) composition distribution of silicon and oxygen along the white arrow in (a), obtained by EDX.

loading rate. The Li compounds in the prepared composite may optimize the charge–discharge properties. A mechanochemically synthesized composite of Si and CuO with a high initial coulombic efficiency of 89.1% was reported in our previous paper[26]. The addition of Li ions is expected to improve the electrical and ionic conductivities of the active material. Moreover, because ceramic CuO and Li_2O are respectively known as non-occlusive and non-conductive materials, they do not function as active materials in the LIB. In this study, the composite, consisting of aggregates of Si, other conductive nanoscale grains, and a Si oxide material produced mechanochemically by grinding was successfully employed as an anode to occlude Li ions with high coulombic efficiency from the first charge–discharge stage. A conductive layer, such as silicon mono-oxide, on Si-Li_2O-CuO composite powder lowers interfacial resistance, stabilizes electrical connections and promotes uniform lithium-ion reactions. It also limits direct electrolyte contact, forming a thinner, more stable SEI that reduces irreversible lithium loss and increases active material utilization during cycling.

Moreover, the plateau in charge–discharge characteristics that appears around 2.3 V at 500 mAh g^{-1} in Fig. 7a is assumed to be the formation of a crystalline $Li_{15}Si_4$ phase. This plateau is thought to be caused by the redox-induced degradation of the active material, and the smaller plateau is thought to indicate a trend toward nano-grain size and homogenization of the grain size of the silicon in the active material. And the oxidation rate is expected to be higher for the complex exposed to air than for the complex not exposed to air; if the plateau around 2.3 V in Fig. 7a is due to the oxide being reduced by Li ions, it is reasonable that the side reaction is greater for the complex exposed to air.

Figures 7b and (c) show the comparison of the composites treated in Ar atmosphere and air, and Si particles as a reference an anode. Figure 7b shows the cycling properties of the reversible capacity for between charge–discharge properties in the voltage range of 1.6–4.2 V at a current density of 3.2 mA/cm^2 (1 C) with $LiCoO_2$ employed as a cathode in a coin cell, and Fig. 7c shows the retention characteristics. The anodes measured were the composite with Si, Li_2O, and CuO particles produced by a mechanochemical process conducted in Ar atmosphere and air (orange circle dots), the composite prepared in Ar atmosphere (red triangle dots), and Si particles as a reference (blue square dots). The anodes with the composite with Si, Li_2O and CuO particles synthesised in Ar atmosphere and air and in Ar atmosphere only, showed a higher retention capacity than the electrodes with only silicon powder. In particular, the composite synthesised in Ar atmosphere and air retained a maintenance factor close to 1.0 at 500 cycles. This result is in contrast to the behavior of bare Si particles, which had a low retention capacity below 50% until 200 cycles. However, the Si and Li or Cu compounds synthesized by grinding this mixture increased the electrical and ionic conductivities in the prepared composite, thereby helping maintain a high capacity over a large number of charge–discharge cycles.

It was also confirmed that the active materials treated only with Ar gas showed a large initial drop with respect to charge–discharge characteristics. This is because the active material treated with only Ar gas is considered to have the same structure as the active material composed of nano-Si, silicate, and conductive alloys, as well as the active material with a large initial drop in charge–discharge cycle characteristics[26].

We postulate that a composite material consisting of a poly–Si, Si oxide, Si–Cu alloy, and Li–silicate oxide will likely yield good performance in terms of the charge–discharge characteristics in an LIB. The alloying of Li and Cu by mechanochemical processing can transform Si into a Si alloy or other oxide compounds, as well as the possibility of improving load properties as batteries (see Fig. S1 in supplementary information). Improvements in the stability of Si anodes have been observed as a result of such individual attempts, leading to improvements in LIB performance[34–36]. We consider that further significant improvement will be obtained from the synergistic effects of two or more approaches simultaneously introduced in one simple operation.

The presence of Li or Cu in the composite is hypothesized to improve the electrical and ionic conductivities of the composite. Thus, impedance measurements were carried out to identify elements that improve the electrical and ionic conductivities. Figure 8 shows the impedance measurement results for the composite with Si, Li_2O, and CuO particles produced by a mechanochemical process conducted in Ar atmosphere and air (orange circle

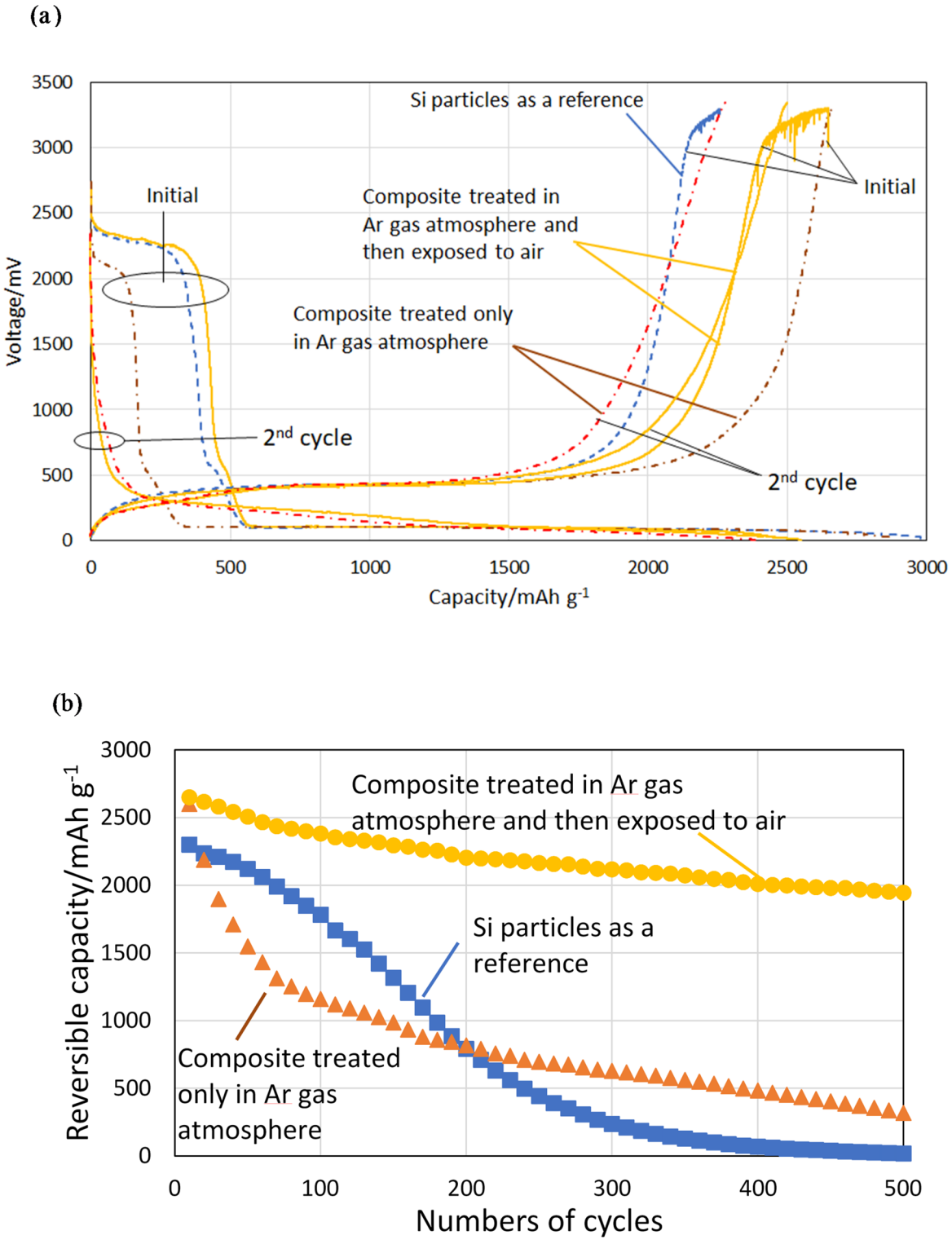

Fig. 7. **(a)** Initial and second charge–discharge properties of the prepared composite with Si, Li_2O, and CuO, and Si particles at loading current density of 3.2 mA/cm^2 (1 C). The capacity (mAh/g) is normalized by the weight of Si in the composite. **(b)** Cycling properties of anodes with the composites treated in Ar atmosphere and air, and Si particles as a reference. **(c)** Cycling properties of the retention based on the data in (b).

dots), the composite prepared in Ar atmosphere (red triangle dots), and Si particles as a reference (blue square dots). The samples were evaluated in a 2032-type coin cell with metal Li foil as the cathode. We could find the composites with Si, Li_2O, and CuO particles have capacitive semicircles of 100 Ω and 200 Ω respectively, and the Si particle has capacitive semicircle of over 5000 Ω. The volume change of Si is larger than that of composite

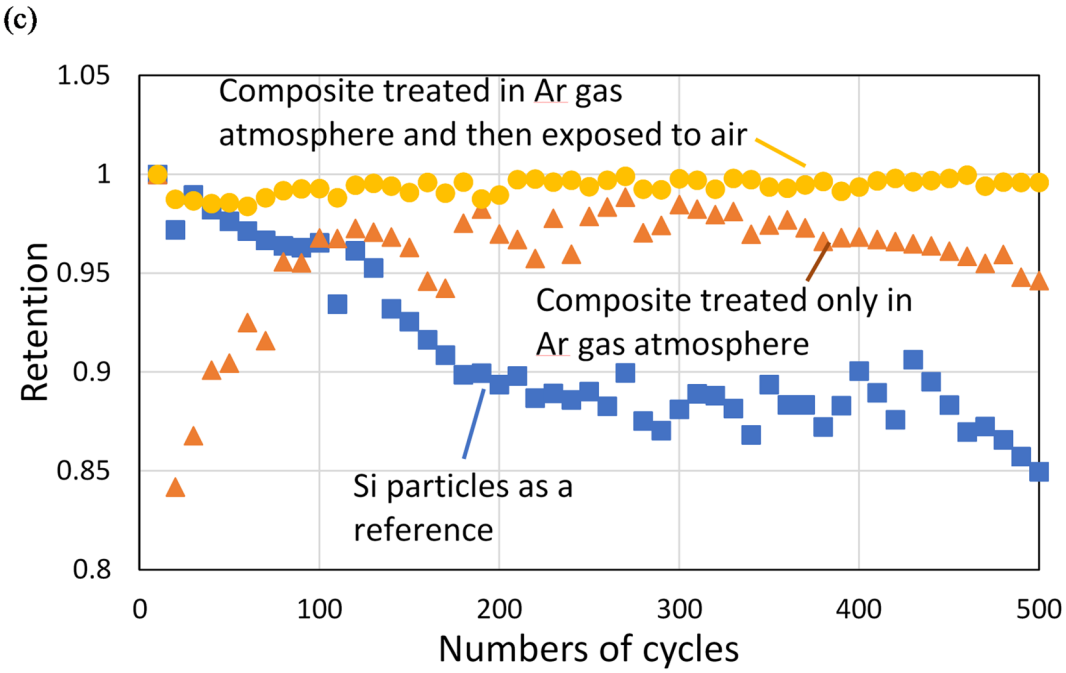

Fig. 7. (continued)

active material, and the solid electrolyte interphase (SEI) will form thicker and the interface resistance of Si will be higher. In addition, the thin oxide film formed on the surface layer of the composite conducted in Ar atmosphere and air bulks up the resistance component, which is thought to have taken the trend shown in Fig. 9.

We observed punctate materials in the composite, leading us to surmise that the composite was a mixture of materials based on compounds of Si, Li_2O, and CuO. Moreover, a major obstacle to achieving satisfactory reversible capacity in practical use lies in the large change in the Si volume observed during charge–discharge operation. However, when observing the cross section of the composite active material before and after the charge–discharge cycle evaluation as shown in Fig. 9, it was confirmed that the active material retained its composition and structure after 500 cycles. It is noteworthy that the shape of the composite and atomic distributions of Si, Li, and Cu were maintained during the testing cycles and no collapse of the structure was observed in the presence of SiO as a buffer matrix. The amorphous structure of SiO[37–40] in the composite is expected to play a role in mitigating the expansion of active materials with nano-Si grains and Li ions. Furthermore, active materials with a structure that protects the surface of the active material are less likely to form non-conductors (SEI) generated in the electrolyte during the charge–discharge process, which has the effect deters the degradation of cycle properties. When the compound formed in Ar atmosphere using a three-dimensional ball mill was further processed in air at a low rotation speed, it is assumed that a layer of altered silicon oxide is formed only on the surface layer of the compound, as shown in Fig. 10, which improves in cycle properties.

The standard motion occurring in a ball mill is cataracting owing to strong mechanical interactions such as impact and compression in Fig. 11, but the cascading of ball groups occurs when two independent axes rotate the vessel in three dimensions. The three-dimensionally ball mill is a combination of the above-mentioned motions, dependent on the rotational speed of the vessel. The material in the vessel is processed in this state. Then, a mechanochemical process involving grinding and re-synthesising multiple submicron-sized granular materials down to the nano scale can occur in the synthesis of complex compound aggregates inside the composite, as shown in Fig. 10. Furthermore, by adjusting the atmosphere inside the vessel and the rotation speed of the vessel, strong frictional forces act between the composites or between them and the ball, producing an effect that alters the particle surface as shown in Fig. 11.

Conclusion

We conclude that the structure of the composite unites the structural features of an active material based on a silicon composite with high retention capacity and cyclic reversible charge properties. The following observations have been made:

A homogeneous dispersion of Cu_3Si nanoscale grains, Si nanoparticles, amorphous SiO, and Si–Li compounds is obtained by a simple cataracting motion of the mechanochemical grinding process. When ground at 300 K in Ar gas, the crystals of both Cu_3Si and Si nanoparticles align randomly.

Our prepared composite shows higher retention capacity and coulombic efficiency (near 100%) than Si alone. The ground samples exhibit higher cycling capability than simple mixtures, and we could show that the existence of a Si–Cu alloy, and SiO and Si–Li compounds in the composite is an important factor for improving cycling performance.

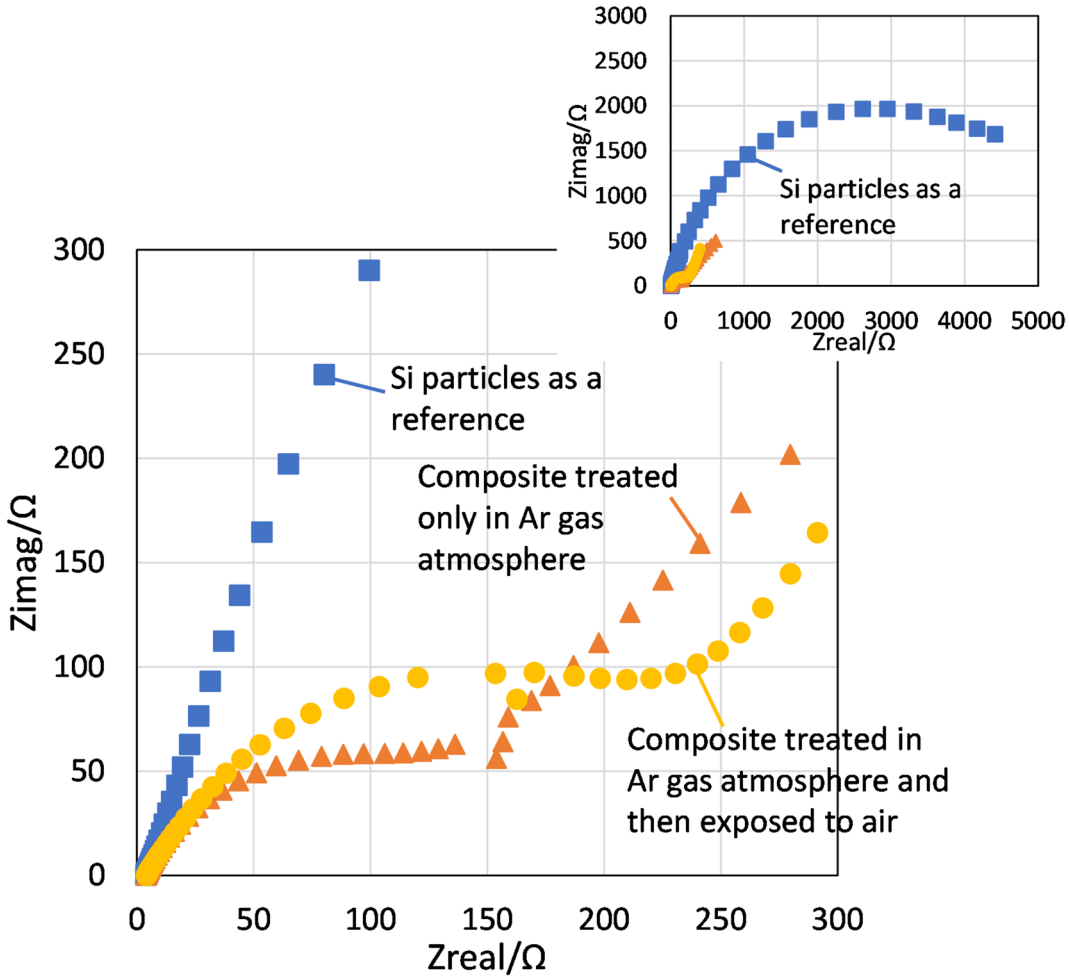

Fig. 8. Impedances of the composite with Si, Li_2O, and CuO, and only Si as a reference. The inset graph shows the curve summary of the Nyquist plot of the reference anode active material with Si particles.

An oxide layer was successfully formed on the surface layer of the composite by an extremely simple process through cascading motion using a three-dimensional ball mill. Furthermore, the silicon oxide exhibited high electrical conductivity and could be shown to be effective in improving cycle properties.

Thus, we have achieved the synthesis of an active composite material serving as an anode in an LIB by a simple mechanochemical grinding process. The successful material preparation for a Si anode this time was performed with a small amount of CuO added for nonstoichiometric reactions, expanding our understanding of mechanochemical phenomena. While optimizing our treatment conditions for Si composite preparation, we are considering different applications of nonstoichiometric reactions to other similar issues.

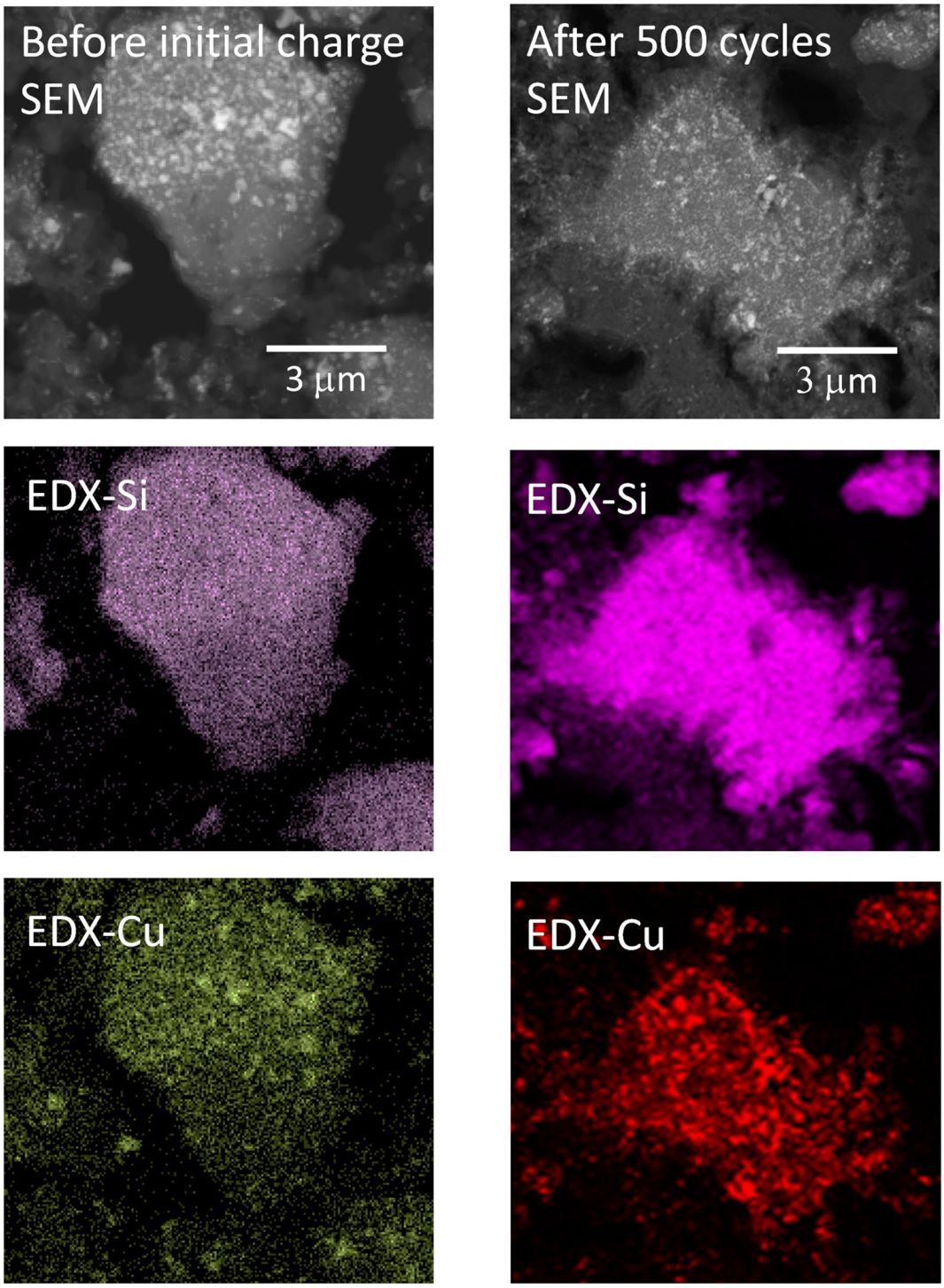

Fig. 9. Cross section images of SEM bright field and EDX distribution map with the composite material having Si and Cu before the initial charge and after 500 cycles.

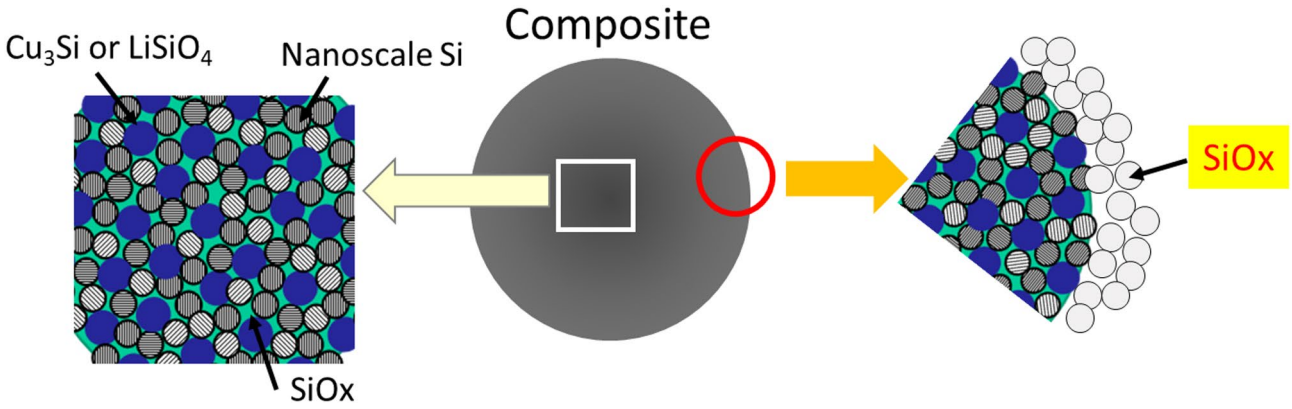

Fig. 10. Distributions of Si, O and Cu determined by EDX, as shown in Figs. 5 and 6 in the composite with Si, Li_2O, and CuO. Cross-sectional view of the composite with Si, Li_2O, and CuO prepared in Ar gas atmosphere and then exposed to air. Silicon oxides distributed around the particles to protect the surface of the active material are less likely to form SEI generated in the electrolyte.

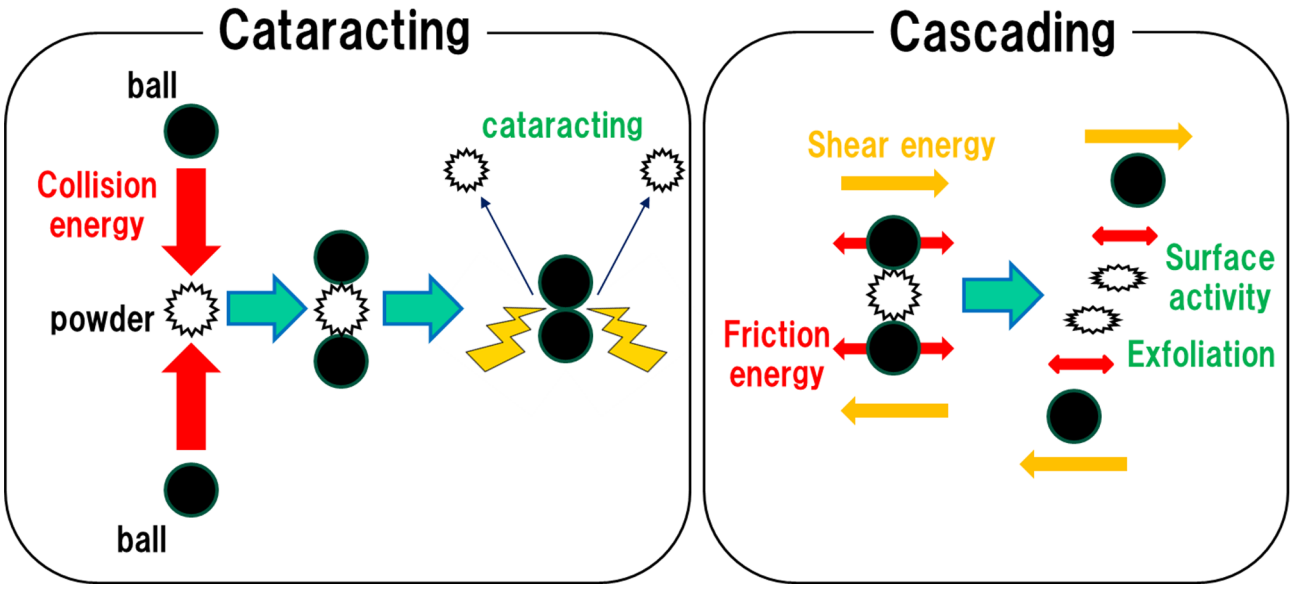

Fig. 11. Model of cataracting and cascading motion in a three-dimensionally driven ball mill.

Data availability

The data that support the findings of this study are available within the article.

Received: 8 September 2024; Accepted: 20 May 2025
Published online: 26 May 2025

References

1. Netz, A., Huggins, R. A. & Weppner, W. The formation and properties of amorphous silicon as negative electrode reactant in lithium systems. *J. Power Sources* **119–121**, 95–100 (2003).
2. Besenhard, J. O. *Handbook of Battery Materials* (Wiley-VCH, 1999).
3. Huggins, R. A. Materials science principles related to alloys of potential use in rechargeable lithium cells. *J. Power Sources*. **26**, 109–120 (1989).
4. Obrovac, M. N. & Krause, L. J. Reversible cycling of crystalline silicon powder. *J. Electrochem. Soc.* **154**, A103–A108 (2007).
5. Liu, X. H. et al. Size-dependent fracture of silicon nanoparticles during lithiation. *ACS Nano*. **6**, 1522–1531 (2012).
6. Zhao, K. et al. Concurrent reaction and plasticity during initial lithiation of crystalline silicon in lithium-ion batteries. *J. Electrochem. Soc.* **159**, A238–A243 (2012).
7. Hu, Y. S. et al. Superior storage performance of a Si@SiO_x/C nanocomposite as anode material for lithium-ion batteries. *Angew Chem. Int. Ed.* **47**, 1645–1649 (2008).
8. Kovalenko, I. et al. A major constituent of brown algae for use in high-capacity Li-ion batteries. *Science* **334**, 6052, 75–79 (2011).
9. Magasinski, A. et al. High-performance lithium-ion anodes using a hierarchical bottom-up approach. *Nat. Mater.* **9**, 353–358 (2010).

10. Szczech, J. R. & Jin, S. Nanostructured silicon for high capacity lithium battery anodes. *Energy Environ. Sci.* **4**, 56–72 (2011).
11. Liu, N. et al. A yolk-shell design for stabilized and scalable Li-ion battery alloy anodes. *Nano Lett.* **12**, 3315–3321 (2012).
12. Hu, L. et al. Si nanoparticle-decorated Si nanowire networks for Li-ion battery anodes. *Chem. Commun.* **47**, 367–369 (2011).
13. Holzapfel, M. et al. Nano silicon for lithium-ion batteries. *Electrochim. Acta*. **52**, 973–978 (2006).
14. McDowell, M. T. et al. Studying the kinetics of crystalline silicon nanoparticle lithiation with in situ transmission electron microscopy. *Adv. Mater.* **24**, 6034–6041 (2012).
15. Yang, J. et al. SiO_x-based anodes for secondary lithium batteries. *Solid State Ionics*. **152–153**, 125–129 (2002).
16. Shimoi, N. & Tanaka, Y. Improvement in Si active material particle performance for lithium-ion batteries by surface modification of an inductivity coupled plasma-chemical vapor deposition. *Electrochim. Acta*. **80**, 227–232 (2012).
17. Hochgatterer, N. S. et al. Silicon/graphite composite electrodes for high-capacity Anodes: influence of binder chemistry on cycling stability. *Electrochem. Solid-State Lett.* **11**, A76–A80 (2008).
18. Jang, B. O. et al. Electrospun Co-Sn alloy/carbon nanofibers composite anode for lithium ion batteries. *J. Alloys Compd.* **574**, 335–340 (2013).
19. Wu, H. et al. Stable cycling of double-walled silicon nanotube battery anodes through solid–electrolyte interphase control. *Nat. Nanotechol.* **7**, 309–315 (2012).
20. Ebner, M. et al. Visualization and quantification of electrochemical and mechanical degradation in Li ion batteries. *Science* **342**, 6159, 716–720 (2013).
21. Li, X. et al. Germanium anode with excellent lithium storage performance in a germanium/lithium–cobalt oxide lithium-ion battery. *ACS Nano*. **9**, 1858–1867 (2015).
22. Wang, K. X. et al. Surface and interface engineering of electrode materials for lithium-ion batteries. *Adv. Mater.* **27**, 527–545 (2015).
23. Jung, S. C. et al. Sodium ion diffusion in Al_2O_3: a distinct perspective compared with lithium ion diffusion. *Nano Lett.* **14**, 6559–6563 (2014).
24. Li, J. et al. Artificial solid electrolyte interphase to address the electrochemical degradation of silicon electrodes. *ACS Appl. Mater. Interfaces*. **6**, 10083–10088 (2014).
25. Lee, D. J. et al. Nitrogen-doped carbon coating for a high-performance SiO anode in lithium-ion batteries. *Electrochem. Commun.* **34**, 98–101 (2013).
26. Shimoi, N. et al. Mechanochemical approaches to employ silicon as a lithium-ion battery anode. *AIP Adv.* **5**, 057142 (2015).
27. Suryanarayana, C. Mechanical alloying and milling. *Prog Mater. Sci.* **46**, 1–184 (2001).
28. Tanaka, Y., Zhang, Q. & Saito, F. Mechanochemical dechlorination of trichlorobenzene on oxide surfaces. *J. Phys. Chem. B*. **107**, 11091–11097 (2003).
29. Beyer, M. K. & Clausen-Schaumann, H. Mechanochemistry: the mechanical activation of covalent bonds. *Chem. Rev.* **105**, 2921–2948 (2005).
30. Welham, N. J. Mechanochemical reduction of $FeTiO_3$ by Si. *J. Alloys Compd.* **274**, 303–307 (1998).
31. Zhang, Q. et al. Sulphidization of metal oxides by means of mechanochemical solid reaction. *Chem. Lett.* **31**, 1094–1095 (2002).
32. Shengqi, X. et al. The reduction of CuO by Si during ball milling. *J. Mater. Sci. Lett.* **15**, 634–635 (1996).
33. Bernard, F., Souha, H. & Gaffet, E. Enhancement of self-sustaining reaction Cu_3Si phase formation starting from mechanically activated powders. *Mater. Sci. Eng. A*. **284**, 301–306 (2000).
34. Hwa, Y. et al. Modified SiO as a high performance anode for Li-ion batteries. *J. Power Sources*. **222**, 129–134 (2013).
35. He, M. et al. Monodisperse antimony nanocrystals for High-Rate Li-ion and Na-ion battery Anodes: nano versus bulk. *Nano Lett.* **14**, 1255–1262 (2014).
36. Larcher, D. et al. Recent findings and prospects in the field of pure metals as negative electrodes for Li-ion batteries. *J. Mater. Chem.* **17**, 3759–3772 (2007).
37. Jolly, F. et al. Temperature effects on the Si/SiO_2 interface defects and suboxide distribution. *J. Non-Cryst Solids*. **245**, 217–223 (1999).
38. Nagao, Y. et al. Structural analysis of pure and electrochemically lithiated SiO using neutron elastic scattering. *J. Electrochem. Soc.* **151**, A1572–A1575 (2004).
39. Hohl, A. et al. An interface clusters mixture model for the structure of amorphous silicon monoxide (SiO). *J. Non-Cryst Solids*. **320**, 255–280 (2003).
40. Mamiya, M. et al. Preparation of fine silicon particles from amorphous silicon monoxide by the disproportionation reaction. *J. Cryst. Growth*. **229**, 457–461 (2001).

Acknowledgements

We kindly thank Kameyama Iron Factory Inc. for their help in the construction and electrochemical measurements of the composite employed in this study.

Author contributions

N.S. wrote the text of the manuscript, H.A. prepared the samples, and M.K. made the measurements and prepared the graphs. All authors reviewed the manuscript.

Funding

We have not received any funding to conduct this study.

Declarations

Competing interests

The authors declare no competing interests.

Additional information

Supplementary Information The online version contains supplementary material available at https://doi.org/10.1038/s41598-025-03505-7.

Correspondence and requests for materials should be addressed to N.S.